Proceedings of the 9th International Conference on Heat Transfer and Fluid Flow (HTFF'22)
Prague, Czech Republic – July 31, 2022 - August 02, 2022
Paper No. HTFF 189
DOI: 10.11159/htff22.189

Natural Circulation in a PWR for a Sinusoidal Heat Input: Analytical Model

Mohammed Abdulrahman
Rochester Institute of Technology
mwacad@rit.edu

Abstract - Natural circulation is a crucial passive heat removal process for all light water reactors. To understand the consequences of decreasing primary coolant inventory on natural circulation, an analytical one-dimensional model has been developed for a sinusoidal input heat distribution, based on solutions to the continuity, momentum and energy equations and expressions for the natural circulation parameters have been derived for PWR plant. The model encompasses all potential types of natural circulation (single-phase, combined single and two-phase, and two-phase). In this paper, it is found that the transition between the different modes of natural circulation with various system inventories is smooth. As the flow mode changes from single-phase (100% mass inventory) to two-phase natural circulation, the loop mass flow rate increases and exhibits a peak within a narrow band of inventory (usually between 60-80%). Also, it is demonstrated that natural circulation in a PWR type system can provide an effective mechanism for the rejection of core decay heat to the secondary over a primary coolant inventory range of 100 to 60%, and a core decay power range of 1.5 to 5% of full power. Comparisons are made between pervious experimental results and prior research and the analytical outcomes are found to be in reasonable accord.

***Keywords*:** Natural circulation; PWR; LOCA; inventory; sinusoidal heat input

1. Introduction

During specific accidents or transients, a light water reactor's natural circulation can offer substantial cooling. For the recirculation of cooled fluid and condensed steam, natural circulation requires just a hydrostatic head differential between the heat source (core) and the heat sink (steam generator). It is noted that one of the prerequisites for an operating licence for a new nuclear power reactor is to conduct a natural circulation test. In LWRs, accidents can occur in a number of ways, i.e., pump seal failure, steam generator tube failure, or safety valves sticking open, and instrument-tube failure, in addition to simple pipe breaks or leaks. Simple loops have been studied in order to better understand the basic phenomena in thermosyphons. Most of the work on thermosyphons has been concerned with single flow path loops. Some applications, for example the cooling systems of pressurized water reactors (PWRs), involve parallel loops.

A survey is presented on the theoretical and experimental work on natural circulation loops. It includes, review papers, experimental studies and modeling methods (analytical and numerical) that deal exclusively with natural circulation flow in nuclear reactor plants. Mckee (1970) presented a review on thermosyphon reboilers [1]. Grief (1988) discussed a number of representative works and programs on natural circulation loops [2]. Other reviews on similar topics had been given by Metrol et al. (1981) [3], Norton and Probert (1982, 1986) [4-5] and Mertol and Grief (1985, 1987) [6-7]. Chato (1963) investigated a parallel-channel system of vertical tubes between two constant-temperature reservoirs. His results show that such systems can exhibit instabilities due to multiple steady-state solutions [8]. Steady-state, transient behaviour and stability characteristics had been investigated in toroidal and vertical loops [9-10], including the effects of a throughflow. This latter case may be important in a nuclear reactor loop when cold makeup water must be added. Some natural circulation loops involve two-phase flows (e. g., thermosyphon reboilers and natural circulation reflux boiling in LWR loops) had been studied by Fernandez [11]. Gillette et al. and Gregory et al. studied the transient behavior and stability of liquid metal fast breeder reactor loops (LMFBRs) [12-13].

PWR nuclear power plant data was introduced [14-15]. These data primarily consist of the temperatures of the hot and cold legs, the pressures of the primary coolant, and the pressures and water levels of the pressurizer and secondary sides of the steam generators. Some characteristics of the transition between single-phase and two-phase natural circulation flows in plants were explored [16] along with some of the events that happened during the accident at the Three Mile Island unit 2 (TMI-2) facility. Yeung and Denver presented nuclear power plant data for natural circulation flows that pre valid at about

0. 1 percent of full power. The power plant is a 2500 MWt PWR with two loops having once-through steam generators [17-18]. The unique relationship that exists between liquid inventory and total loop flow rate, was also shown by computer code (RELAP 5) computations [19]. A similar effect was observed in an OTSG loop [20] during a small break transient. Duffey and Sursock (1987) created a theoretical model to examine natural circulation phenomena pertinent to small breaks and transients for pressurized water reactors (PWRs) and boiling water reactors (BWRs), as well as analyzed the pertinent experimental data.

The physics of circulation process is a manometric balance between the hydrostatic head in the downcomer driving the core inlet flow, and the pressure losses incurred in venting the resulting two-phase flow from the core outlet to the heat exchanger [21-22]. Abdulrahman et al. (2021) have investigated theoretically the natural circulation phenomena in a PWR during a small break loss of coolant accident [23-25]. They have derived analytical equations for mass flow rate and inlet and outlet core temperatures for single-phase, two-phase, and combined single and two-phase flow with uniform core heat distribution.

This work considers the whole spectrum from liquid to pure steam circulation, for the conditions relevant to PWR accidents and transients for sinusoidal core heat distribution. A fundamental tenet of this work is that the entire circulation process can be treated as quasi-steady. The inventory loss rate through the break is sufficiently small that flashing and acceleration effects are negligible. This has been confirmed experimentally [26] by superimposing a small break on a PWR loop in natural circulation and showing that the loop floe response duplicates that obtained in steady-state tests for a range of inventories. Not only does this hypothesis greatly simplify the theory, it enables the controlling phenomena to be clearly understood and described analytically.

2. Natural Circulation in a Steady State One-Dimensional Flow

The conservation equations of mass, momentum, and energy for a steady state one-dimensional flow in the z-direction, are [2];

$$\frac{dv}{dz} = -\frac{v}{\rho}\frac{d\rho}{dz} \tag{1}$$

$$\rho v \frac{dv}{dz} = -\frac{dP}{dz} - F_z - \rho g \cos(\theta) \tag{2}$$

$$\rho v A \frac{dh}{dz} = -\frac{dq}{dz} \tag{3}$$

By solving Eqs. (1) and (2), the mass flow rate can be found as [23];

$$\dot{m} = \frac{\widehat{m}}{\bar{\rho}_o}\sqrt{\rho_l\,(\bar{\rho}_2 - \bar{\rho}_1)\frac{\bar{f}_o}{\bar{f}}} \tag{4}$$

where,

$$\widehat{m}^2 = \frac{2\,g\,L_z\,\overline{D}\,\bar{\rho}_o^2\bar{A}^2}{4\,\bar{f}_o L_t} \tag{5}$$

Note that $\widehat{m}$ has the dimensions of flow rate and $\bar{f}_o$ and $\bar{\rho}_o$ are respectively the overall system average friction coefficient and density corresponding to the conditions at the beginning of natural circulation. Each component of the loop's energy in Eq. (3) may be expressed independently. For the heated part, it is determined by the distribution of the input power. It is widely established that the power distribution inside a typical PWR core is not uniform. In this paper, the distribution is assumed to be sinusoidal. Hence, Eq. (3) takes the form;

$$\dot{m}\frac{dh}{dz} = \begin{cases} -\dfrac{dq}{dz} = q_c' \sin\dfrac{\pi\, z}{L_c} & \text{(heat source)} \quad (6a) \\ -\bar{U}\pi D_s n(T_s - T_{sec}) & \text{(heat sink)} \quad (6b) \\ 0 & \text{(insulated pipes)} \quad (6c) \end{cases}$$

The term q_c' in Eq. (6a) can be obtained from the total input power of the core, Q_t, thus;

$$Q_t = \int_0^{L_c} q_c' \sin\frac{\pi\, z}{L_c}\, dz = 2\frac{L_c}{\pi} q_c'$$

hence;

$$q_c' = \frac{\pi}{2L_c} Q_t \tag{7}$$

For incompressible single-phase flow, the density ρ at any temperature T is determined from;

$$\rho = \rho_l(1 + \beta T_l) - \rho_l \beta T \tag{8}$$

2.1. Single-Phase loop flow

In single-phase, $dh = C\, dT$, and Eqs. (6) can be written as;

$$\dot{m}\, C\frac{dT}{dz} = \begin{cases} q_c' \sin\dfrac{\pi\, z}{L_c} & \text{(heat source)} \quad (9a) \\ -\bar{U}_1\pi D_s n(T_s - T_{sec}) & \text{(heat sink)} \quad (9b) \\ 0 & \text{(insulated pipes)} \quad (9c) \end{cases}$$

By solving Eqs. (9a) and (9b), the profiles of the core temperature (T_c) and the primary side of the steam generator temperature (T_s) are respectively determined as;

$$T_c = T_i + \frac{Q_t}{2\, \dot{m}\, C}\left[1 - cos\frac{\pi\, z}{L_c}\right] \qquad (0 \le z \le L_c) \tag{10}$$

$$T_s = T_{sec} + (T_o - T_{sec})e^{-\frac{\bar{U}_1 \pi D_s n}{\dot{m}\, C} z} \qquad (0 \le z \le L_s) \tag{11}$$

where z, is the distance measured from the bottom of the reactor core in Eq. (10) and measured from the bottom of the primary side of the hot leg of the steam generator in Eq. (11). The solution of Eq. (9c) results in a temperature distribution that is uniform across the connecting pipes, where the outlet temperature of the core (T_o) is the same as the inlet temperature of the steam generator and the outlet temperature of the steam generator is the same as the inlet temperature of the core (T_i). The outlet temperature of the core (T_o) is obtained by substituting $z = L_c$ into Eq. (10), and the inlet temperature of the core (T_i) is obtained by substituting $z = L_s/2$ into Eq. (11).

The value of $\bar{\rho}_1$ in Eq. (4) is calculated by volume averaging the densities on the up-flow side of the PWR system components, and the value of $\bar{\rho}_2$ is constant at a temperature T_i.

$$\bar{\rho}_1 = \frac{\bar{\rho}_c V_c + \bar{\rho}_u V_u + \bar{\rho}_s \frac{V_s}{2}}{V_1} \tag{12}$$

$$\bar{\rho}_2 = \rho_l(1 + \beta T_l) - \rho_l \beta T_i \tag{13}$$

where;

$$\bar{\rho}_c = \frac{\int_0^{L_c} \rho_c dz}{L_c} = \rho_l(1+\beta T_l) - \rho_l\beta\left(\frac{T_i + T_o}{2}\right) \tag{14}$$

$$\bar{\rho}_u = \rho_u = \rho_l(1+\beta T_l) - \rho_l\beta T_o \tag{15}$$

$$\bar{\rho}_s = \frac{\int_0^{\frac{L_s}{2}} \rho_s\, dz}{\frac{L_s}{2}} = \rho_l(1+\beta T_l) - \rho_l\beta T_{sec} + \frac{\rho_l\beta(T_0 - T_{sec})\dot{m}C}{\frac{L_s}{2}\bar{U}_1\pi D_s n}\left\{e^{-\frac{\bar{U}_1\pi D_s n}{\dot{m}C}\frac{L_s}{2}} - 1\right\} \tag{16}$$

$$V_1 = V_c + V_u + \frac{V_s}{2} \tag{17}$$

2.2. Combined single and two-phase loop flow

The energy equations for non-boiling and boiling heights of each component in the PWR are respectively expressed as;

$$\dot{m}\, C\frac{dT}{dz} = \begin{cases} q_c' \sin\frac{\pi\, z}{L_c} & \text{(Non Boiling height of heat source)} \quad (18a) \\ -\bar{U}_1\,\pi\, D_s n(T_s - T_{sec}) & \text{(Non Boiling length of steam generator)} \quad (18b) \\ 0 & \text{(Cold leg pipe)} \quad (18c) \end{cases}$$

$$\dot{m}\frac{dh}{dz} = \begin{cases} q_c' \sin\frac{\pi\, z}{L_c} & \text{(Boiling height of heat source)} \quad (19a) \\ -\bar{U}_2\,\pi\, D_s n(T_{sat} - T_{sec}) & \text{(Boiling length of steam generator)} \quad (19b) \\ 0 & \text{(hot leg pipe)} \quad (19c) \end{cases}$$

By solving Eqs. (18) and (19), the temperature profiles of the core (T_c) and the primary side of the steam generator (T_s) for non-boiling regions as well as their quality profiles for boiling regions are found as follows;

$$T_c = T_i + \frac{Q_t}{2\,\dot{m}\,C}\left[1 - cos\frac{\pi\, z}{L_c}\right] \qquad 0 \le z \le L_c' \tag{20}$$

$$T_s = T_{sec} + (T_{sat} - T_{sec})\, e^{-\frac{\bar{U}_1\pi D_s n}{\dot{m}C}(z - L_s + L_s')} \qquad (L_s - L_s') \le z \le L_s \tag{21}$$

$$x_c = \frac{Q_t}{2\,\dot{m}\, h_{fg}}\left[\cos(\pi L_c^*) - \cos(\frac{\pi\, z}{L_c})\right] \qquad (L_c' \le z \le L_c) \tag{22}$$

$$x_s = x_o - \frac{\bar{U}_2\pi D_s n(T_{sat} - T_{sec})}{\dot{m}\, h_{fg}} z \qquad (0 \le z \le (L_s - L_s')) \tag{23}$$

The solution of Eq. (18c) results in uniform temperature distribution in the cold leg pipe, whereas the solution of Eq. (19c) results in uniform enthalpy distribution and hence in uniform quality distribution in the hot leg pipe. The temperature and quality profiles described by Eqs. (20) through (23) are used to obtain the density distribution for each elemnet of a PWR loop.

For the core:

$$\bar{\rho}_c = \bar{\rho}_{c1} + \bar{\rho}_{c2} \tag{24}$$

where;

$$\bar{\rho}_{c1} = \left(a + bT_i + \frac{bQ_t}{2\,\dot{m}C}\right)L_c^* - \frac{bQ_t}{2\,\pi\,\dot{m}C}\sin(\pi L_c^*) \tag{25}$$

$$\bar{\rho}_{c2} = \begin{cases} \dfrac{2}{\pi\sqrt{y_3^2 - y_4^2}}\left[\dfrac{\pi}{2} - tan^{-1}\left\{\dfrac{y_3 + y_4}{\sqrt{y_3^2 - y_4^2}}tan\left(\dfrac{\pi L_c^*}{2}\right)\right\}\right] & (for\ y_3^2 > y_4^4), \quad (26a) \\ \dfrac{1}{\pi\sqrt{y_4^2 - y_3^2}}ln\left|\dfrac{\dfrac{\sqrt{y_4^2 - y_3^2}}{tan\left(\frac{\pi L_c^*}{2}\right)} + (y_3 + y_4)}{\dfrac{\sqrt{y_4^2 - y_3^2}}{tan\left(\frac{\pi L_c^*}{2}\right)} - (y_3 + y_4)}\right| & for(y_3^2 < y_4^4) \quad (26b) \end{cases}$$

where;

$$y_3 = v_f + \frac{v_{fg}Q_t}{2\dot{m}h_{fg}}\cos(\pi L_c^*) \tag{27}$$

$$y_4 = \frac{v_{fg}Q_t}{2\,\dot{m}\,h_{fg}} \tag{28}$$

For the hot leg and upper plenum:

$$\bar{\rho}_u = \frac{1}{v_f + v_{fg}\,x_o} \tag{29}$$

For the steam generator:

$$\bar{\rho}_s = \bar{\rho}_{s2} + \bar{\rho}_{s1} \tag{30}$$

where;

$$\bar{\rho}_{s2} = \frac{\int_0^{L_s - L_s'} \rho_{s2}\,dz}{\frac{L_s}{2}} = \frac{2\,\dot{m}\,h_{fg}}{v_{fg}\bar{U}_2\pi D_s n(T_{sat} - T_{sec})L_s}ln\left[\frac{v_f + v_{fg}\,x_o}{v_f + v_{fg}\,x_o - \dfrac{v_{fg}\bar{U}_2\pi D_s n(T_{sat} - T_{sec})(L_s - L_s')}{\dot{m}\,h_{fg}}}\right] \tag{31}$$

$$\bar{\rho}_{s1} = \frac{\int_{L_s - L_s'}^{L_s/2} \rho_{s1}\, dz}{\frac{L_s}{2}}$$

$$= (2L_S^* - 1)\left[a + b\,T_{sec} - \frac{b(T_{sat} - T_{sec})C\,\dot{m}}{\bar{U}_1 \pi D_s n(L_s' - \frac{L_s}{2})}\right]\left\{e^{-\frac{\bar{U}_1 \pi D_s n}{\dot{m}C}(L_s' - \frac{L_s}{2})} - 1\right\} \tag{32}$$

$$\bar{\rho}_2 = a + b\left[T_{sec} + (T_{sat} - T_{\mathrm{sec}})e^{-\frac{\bar{U}_1 \pi D_s n}{\dot{m}C}\left(L_s' - \frac{L_s}{2}\right)}\right] \tag{33}$$

To accurately analyse the driving head in a reactor with natural circulation, it is important to determine the non-boiling heights in the channels of the core and steam generator and the average overall heat transfer coefficient of single- and two-phase flow in the channels of steam generator. The non-boiling height of the core L_c' is defined as the height at which the coolant becomes saturated. The remainder of the channel, where boiling occurs, is known as the boiling height, $L_c - L_c'$. Some subcooled boiling occurs in L_c', but it will have minimal impact on the density and can be neglected. The ratio L_c'/L_c may be calculated using the ratio of sensible heat (q_s) contributed to total heat (Q_t) added in the channel [5].

$$\frac{q_s}{Q_t} = \frac{\dot{m}(h_f - h_i)}{Q_t} = \frac{\int_0^{L_c'} q_c' \sin\left(\frac{\pi\, z}{L_c}\right) dz}{Q_t} = \frac{1}{2}\left(1 - \cos(\pi \frac{L_c'}{L_c})\right) \tag{34}$$

hence;

$$L_c^* = \frac{L_c'}{L_c} = \frac{1}{\pi}\cos^{-1}\left[1 - \frac{2\,\dot{m}(h_f - h_i)}{Q_t}\right] \tag{35}$$

Similarly, for the primary side of the steam generator, the non-boiling length is L_s', and the boiling length is $L_s - L_s'$. L_s', can be evaluated by setting $x_s = 0$ at $z = L_s - L_s'$, thus;

$$L_s' = L_s - \frac{x_o\,\dot{m}\,h_{fg}}{\bar{U}_2 \pi D_s n(T_{sat} - T_{sec})} \tag{36}$$

2.3. Two-phase loop flow

In natural circulation, the two-phase mode is considered to commence when the bubbly flow enters the down-flow side of the steam generator and exit pipe. Using the boundary conditions ($x = x_i$ at $z = 0$ and $x = x_o$ at $z = L_c$) established in the preceding section, the following equations are derived for the average densities of each element;

$$\bar{\rho}_c = \frac{1}{\sqrt{y_7^2 - y_8^2}} \tag{37}$$

where;

$$y_7 = v_f + v_{fg}x_i + \frac{v_{fg}Q_t}{2\,\dot{m}\,h_{fg}}$$

$$y_8 = \frac{\upsilon_{fg} Q_t}{2\, \dot{m} h_{fg}}$$

$$\bar{\rho}_u = \frac{1}{\upsilon_f + \upsilon_{fg}\, x_o} \quad (38)$$

$$\bar{\rho}_s = \frac{2\dot{m}\, h_{fg}}{\upsilon_{fg}\, \overline{U}_2\, \pi\, D_s\, n\, (T_{sat} - T_{sec}) L_s}\, ln\left[\frac{\upsilon_f + \upsilon_{fg}\, x_o}{\upsilon_f + \upsilon_{fg}\, x_o - \frac{\upsilon_{fg} \overline{U}_2 \pi D_s n (T_{sat} - T_{sec})}{\dot{m}\, h_{fg}} \frac{L_s}{2}}\right] \quad (39)$$

$$\bar{\rho}_2 = \frac{1}{\upsilon_f + \upsilon_{fg}\, x_i} \quad (40)$$

2.4. Overall heat transfer coefficient

The average overall heat transfer coefficient for single-phase flow, $\overline{U}_1$, and two-phase flow, $\overline{U}_2$ are determined from [3];

$$\overline{U}_1 = \frac{1}{\left(0.023\, Re^{0.8} Pr^{0.3} \frac{k}{d_e}\right)} + \frac{A_i}{A_o (2.5551 \times 10^{-3} e^{0.6446133P} (T_{bulk} - T_{sec})^3)} \quad (41)$$

$$\overline{U}_2 = \frac{1}{(2.5551 \times 10^{-3} e^{0.6446133P} (T_{sat} - T_{sec})^3)} + \frac{A_i}{A_o (2.5551 \times 10^{-3} e^{0.6446133P_{sec}} (T_{sat} - T_{sec})^3)} \quad (42)$$

2.5. Inventory

The fractional mass inventory, *I*, can be written as;

$$I = \frac{M}{M_o} = \frac{\bar{\rho} \forall}{\bar{\rho}_o \forall_o} \quad (43)$$

where M_o and $\bar{\rho}_o$ are the overall fluid mass and system average fluid density corresponding to the conditions at the beginning of natural circulation, and $\bar{\rho}$ is the overall system average fluid density at a given primary pressure. For single-phase flow, the average density of the system will be taken as the density at the bulk temperature (T_{bulk}). The initial loss of coolant mainly produces a drop in fluid level in the vessel upper plenum above the hot leg, so that the volume of the subcooled liquid will decrease by decreasing the primary pressure. The volume decrement progresses to the level of the hot leg, where two-phase flow begins. For two-phase flow, the average volume of the system, $\forall$, will be the same as the total system volume, $\forall_o$, because of existance of saturated vapor, thus;

$$I = \frac{\bar{\rho}}{\bar{\rho}_o} \quad (44)$$

where;

$$\bar{\rho} = \frac{\bar{\rho}_c V_c + \bar{\rho}_u V_u + \bar{\rho}_s \frac{V_s}{2} + \bar{\rho}_2 V_2}{V_1 + V_2} \quad (45)$$

3. Results

It is essential to understand that natural circulation parameter values are determined iteratively. At a particular power Q_t, the values of ρ_o and f_o are determined while the inventory is at 100% and at a specified initial primary pressure (P_o=11.2 MPa). Table 1 contains the values of $\bar{\rho}_o$ and $\bar{f}_o$ for each core power, Q_t.

Table 1: Values of $\bar{\rho}_o$ and $\bar{f}_o$ as a function of core power.

Q_t (KW)	30	60	100
$\bar{\rho}_o$	743.2258	734.6119	730.6987
$\bar{f}_o$	4.847×10^{-3}	4.614×10^{-3}	4.462×10^{-3}

The predictions of the PWR model described in this paper are compared with experimental data from the Semiscale facility [28]. The Mod-2A system was designed as a small-scale model of the primary system of a four loop PWR nuclear generating plant. The system incorporates the major components of a PWR including steam generators, vessel, pumps, pressurizer, and loop piping. An "intact" loop is scaled to simulate three unbroken loops in a PWR and contains 75% of the total loop volume, while a broken loop simulates the single loop, in which a break is postulated to occur in a PWR and contains 25% of the total loop volume. The calculations are done assuming the flow in the broken loop to be essentially stalled (as observed experimentally [29]). Thus, the broken loop acts as a "dead volume". The normalization of the volumes (V_c, V_u, V_s and V_2) therefore refer to volumes of the intact loop relative to the total loops. The experiments on Semiscale Mod-2A system were conducted at three different steady-state powers (30, 60 and 100 KW). Relevant data concerning the Semiscale Mod-2A system are obtained or evaluated from information contained in previous literature [27-28, 30, 5-7]. A summary is presented in table 2 below.

Table 2: Summary of the design and operating data for the Semiscale model.

Parameter	Data	Parameter	Data	Parameter	Data
A_i	3.05×10^{-4} m^2	L_s	20 m	P_{sec}	6 MPa
A_o	3.87×10^{-4} m^2	$\forall_o$	0.165 m^3	T_{sec}	275.64 °C
D_s	0.0222 m	V_c	0.06	T_1	T_{bulk}
t_w	0.00124 m	V_u	0.18	ρ_1	ρ_{bulk}
n	6	V_s	0.22	$\hat{m}$	1.35 Kg/Sec
L_c	3.66 m	V_{cl}	0.29	full core power (scaled)	2 MW

The comparisons of the results of this paper with experimental and theoretical results of previous works on mass flow rate as a function of inventory are shown in Figs. 1-3. These include the experimental data from Semiscale Mod-2A system, results of RELAP5 code, results of Duffey and Sursock [30] analysis and the results of analysis carried out by this paper. An examination of Figs. 1-3 reveals that the present analysis, when compared to the experimental data, predicts the behavior qualitatively and quantitatively more closely than either RELAP5 or Duffey and Sursock. This agreement can be seen to cover the whole range of flow, namely single-phase, combined single and two-phase, and two-phase. The maximum errors, for three power levels, are summarized in Table 3. In particular, it should be noted that the model is capable of predicting both the peak flow and the corresponding inventory with reasonable accuracy. In addition, the present theory captures the correct trend of mass flow rate for the whole range of inventory.

Table 3: Maximum absolute errors between experimental and theoretical results of inventory versus mass flow rate.

	Q_t = 30 kW	Q_t = 60 kW	Q_t = 100 kW
RELAP5 [21]	6.03	6.5	2.1
Duffey and Sursock [30]	15.1	5.5	4.2
Present theory	4.63	5.15	1.64

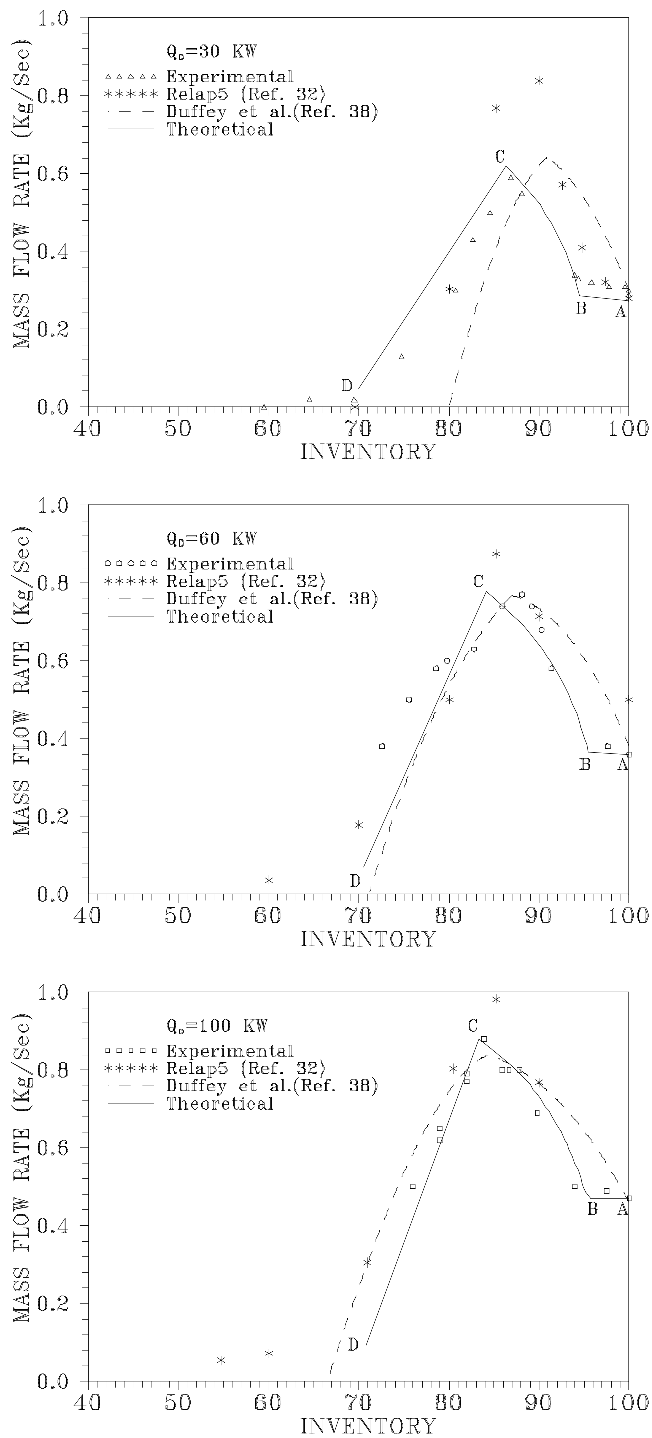

Fig. 1: Comparison of theory with Semiscale PWR data and previous works for Mass flow rate versus Inventory curve.

In the single-phase region, as inventory is reduced, the mass flow remains relatively constant. Beyond the single-phase region, the bouncy force is enhanced progressively, with accelerated vigor as the quality in the hot leg increases while the flow in the cold leg remains single-phase. As the up-flow side of steam generator is filled with two-phase flow (point C in Figs. 1-3), the bouncy force is at a maximum where it gives rise to the maximum flow rate. Beyond point C, the bouncy force with inventory loss, is progressively reduced since two-phase flow develops in the down-flow side of steam generator. This results in continuous and steep reduction in mass flow rate.

4. Conclusions

For sinusoidal heat input, an analytical one-dimensional model was developed based on solutions to continuity, momentum, and energy equations, and formulations for the natural circulation parameters of a PWR plant were produced. By comparing theoretical and experimental data, it was shown that a simple analytical model is capable of predicting the quasi steady-state behaviour during a small LOCA break or loss of pumped flow transient. This work demonstrated that natural circulation in a PWR type system can provide an effective mechanism for the rejection of core decay heat to the secondary over a primary coolant inventory range of 100 to 60% and a core decay power range of 1.5 to 5% of full power. Natural circulation flow rates in PWRs are strongly dependent on liquid inventory, and weakly dependent on power level. The flow rate of a PWR system exhibits a peak within a narrow band of inventory (usually between 60-80%). For a constant steam generator heat sink and slowly decaying core power, quasi stable modes of single-phase, combined single and two-phase, two-phase and reflux condensation can be established, depending on system inventory. The transition between the different modes of natural circulation with various system inventories is smooth.

Abbreviations

Symbol	Definition
A	cross-sectional area of the flow channel
$\bar{A}$	average cross-sectional area of the flow channel
C	specific heat capacity
d_e	equivalent diameter of flow channel
$\bar{D}$	average diameter of the flow channel
D_s	steam generator diameter
$\bar{f}$	average friction factor
g	gravitational acceleration
h	specific enthalpy
h_f	saturated liquid specific enthalpy
h_{fg}	latent heat of vaporization
k	fluid thermal conductivity
L_c	length of the core
n	number of primary tubes of steam generator
P	primary pressure
P_{sec}	pressure in the secondary side of steam generator in MPa
Pr	Prandtle number
q	heat added to (or rejected from) the coolant
Re	Reynolds number
T	fluid temperature
T_i	core inlet temperature
T_o	outlet temperature of the core
T_s	steam generator temperature of the primary side
T_{sat}	saturated temperature
T_{sec}	steam generator temperature of the secondary side
$\bar{U}$	average value of the overall heat transfer coefficient
$\bar{U}_1$	average overall single-phase heat transfer coefficient

$\bar{U}_2$	average overall two-phase heat transfer coefficient
v	flow velocity
v_f	saturated liquid specific volume
V_c	volume of the core
V_u	volume of the sum of the hot leg and upper plenum
V_s	volume of the steam generator

Creek Symbol

β	volume expansion coefficient
ρ	fluid density
ρ_l	density reference value that is evaluated at some reference temperature T_l
$\bar{\rho}_1$	average density of the up-flow side
$\bar{\rho}_2$	average density of the down-flow side
$\bar{\rho}_c$	average density of the core
$\bar{\rho}_{c1\emptyset}$	average core density for single-phase
$\bar{\rho}_{c2\emptyset}$	average core density for two-phase
$\bar{\rho}_s$	average density of the steam generator
$\bar{\rho}_{s1}$	average steam generator density for single-phase
$\bar{\rho}_{s2}$	average steam generator density for two-phase
$\bar{\rho}_u$	average density of the sum of the hot leg and upper plenum

References

[1] H. R. McKee, “Thermosyphon reboilers-a review,” *Ind. and Eng. Chem.*, vol. 62, pp. 76-82, 1970.

[2] R. Greif, “Natural circulation loops,” *J. Heat Transfer*, vol. 110, pp. 1243-1258, 1988.

[3] A. Mertol, W. Place, T. Webster, and R. Greif, “Detailed loop model (DLM) analysis of liquid solar thermosyphon with heat exchangers,” *Solar Energy*, vol. 27, pp. 367-386, 1981.

[4] B. Norton, and S. D. Probert, “Natural circulation solar energy stimulated systems for heating water,” *Applied Energy*, vol. 11, pp. 167-196, 1982.

[5] B. Norton, and S. D. Probert, “Thermosyphon solar energy water heaters,” in *Advances in Solar Energy,* K. W. Boer, ed. American Solar Energy Society, Boulder, CO, vol. 3, 1986, pp. 125-170.

[6] A. Mertol, and R. Greif, “A review of natural circulation loops,” in *Natural convection*, S. Kakac, W. Aung, and R. Viskanta, eds., Hemispere, New York, 1985, pp. 1033-1071.

[7] A. Mertol, and R. Greif, “Review of thermosyphon solar water heaters,” in *Solar Energy_Utilization,* H. Yuncu, E. Paykoc, and Y. Yener, eds., Martinus Nijhoff, Amstrdam, 1987, pp. 537-569.

[8] J. C. Chato, “Natural convection flows in parallel- channel systems,” *J. Heat Transfer*, vol. 85, pp. 339-345, 1963.

[9] P. Welander, “On the oscillatory instability of a differentially heated fluid loop,” *Journal Fluid Mechanics*, vol. 29, pp. 17-30, 1967.

[10] H. F. Creveling, J. F. DePaz, J. Y. Baladi, and R. J. Schoenhais, “Stability characteristics of a single-phase free convection loop,” *Journal Fluid Mechanics*, vol. 67, pp. 65-84, 1975.

[11] Y. Zvirin, and R. Greif, “Transient behavior of natural circulation loops: Two vertical branches with point heat source and sink,” *International Journal Heat Mass Transfer*, vol. 22, pp. 499-504, 1979.

[12] R. Greif, Y. Zvirin, and A. Mertol, “The transient and stability behavior of a natural circulation loop,” *ASME Journal Heat Transfer*, vol. 101, pp. 684-688, 1979.

[13] R. T. Fernandez, J. P. Sursock and R. L. Kiang, “Reflux boiling heat removal in a scaled TMI-2 system test facility,” in *Proceedings of the ANS/ENS Thermal Reactor Safety Meeting*, Knoxville, Tenn, April, 1980.

[14] J. L. Gillette, R. M. Singer, J. V. Tokar, and J. E. Sullivan, “Experimental study of the transition from forced to natural circulation in EBR-II at low pressure and flow,” *ASME*, No. 79-HT-10, 1979.

[15] C. V. Gregory, R. Bell, G. Brown, C. W. Dawson, J. D. C. Henderson, and R. Hampshire, "Natural circulation studies in support of the Dounreay prototype fast reactor(PFR)," in *Proceedings of the ANS/ENS International Meeting On Fast Reactor Safety Technology*, Seattle, Washington, Aug. 1979.

[16] US Nuclear Regulatory Commission, "Generic evaluation of feedwater transients and small-break loss-of-coolant accidents in Westinghouse-designed operating plants," in *Natural circulation*, NUREG-0611. Jan. 1980.

[17] US Nuclear Regulatory Commission, "Generic evaluation of transients and small-break loss-of-coolant accidents in Combustion Engineering-designed operating plants," in *Natural circulation*, NUREG-0635. Jan. 1980.

[18] US Nuclear Regulatory Commission, "Generic evaluation of small-break loss-of-coolant accident behavior in Babcock & Wilcox designed 177-FA operating plant," in *NUREG-0565*, Jan. 1980.

[19] M. R. Yeung, A. H. Meadows, and K. W. Turner, "Reactor coolant system coast down and natural circulation," in *Proceedings of the ANS/ENS Thermal Reactor Safety Meeting*, Knoxville, T, Apr. 1980.

[20] D. J. Denver, J. F. Harrison, Jr and N. G. Trikouros, "RETRAN natural circulation analysis during the Three Mile Island unit 2 accident," in *Proceedings of the ANS/ENS Thermal reactor safety meeting*, Tenn, April, 1980.

[21] L. N. Kmetyk, RELAP-5 assessment, *Conclusions and user guidelines*. NRC report, Sandia National Lab., NUREG / CR-3936 (October 1984).

[22] D. P. Birmingham, R. L. Black and G. C. Rush, "An experimental study of the application of abnormal transient operating guidelines (ATOG) to the Babcock and Wilcox steam supply system during a small break loss-of-coolant accident," in *Proceedings of the 23rd ASME / AIChE / ANS National heat transfer conf*erence, Denver, Colorado, 1985.

[23] M. W. Abdulrahman, M. M. Saleh, and J. Anand "Single-Phase Natural Circulation in a PWR during a Loss of Coolant Accident", in *Proceedings of the 7th International Conference on Fluid Flow, Heat and Mass Transfer (FFHMT'20),* Niagara Falls, Canada, 2020.

[24] M. W. Abdulrahman, M. M. Saleh, and J. Anand "Natural Circulation in a Pressurized Water Reactor with a Combined Single and Two-Phase Mode", in *Proceedings of the 7th International Conference on Fluid Flow, Heat and Mass Transfer (FFHMT'20),* Niagara Falls, Canada, 2020.

[25] M. W. Abdulrahman, and M. M. Saleh, "Two-Phase Flow in the Natural Circulation of a Pressurized Water Reactor", in *Proceedings of the 7th International Conference on Fluid Flow, Heat and Mass Transfer (FFHMT'20),* Niagara Falls, Canada, 2020.

[26] L. W. Ward, "Simplified small-break blowdown models," *Trans. Am. Nucl. Soc.*, vol. 18, pp. 232, 1974.

[27] D. J. Shimeck and G. W. Johnsen, "Natural circulation cooling in a pressurized water reactor geometry under accident-induced conditions," *Nucl. Sci. Engrg.*, vol. 88, pp. 311-320, 1984.

[28] G. G. Loomis and K. Soda, *Results of the Semiscale Mod-2A natural circulation experiments*. NRC Report, Idaho National Engineering Lab., NUREG/CR-2335, September, 1982.

[29] L. E. Hochreiter, E. R. Rosal, S. D. Rupprecht, B. R. Sinwell, J. T. Dederer, K. J. Kovdalski, S. Wong and R. Quaglia, *PWR Flecht Seaset systems-effects natural circulation and reflux condensation data evaluation and analysis report*. EPRI/NRC/Westinghouse Report, Westinghouse Electric Corporation, NP-3497 (February).

[30] R. B. Duffey and J. P. Sursock, "Natural circulation phenomena to small breaks and transients," vol. 102, pp. 115-128, 1987.